

Uplink Multiplexing of eMBB/URLLC Services Assisted by Reconfigurable Intelligent Surfaces

João Henrique Inacio de Souza, Victor Croisfelt, Radosław Kotaba, Taufik Abrão,
and Petar Popovski

Abstract

This letter proposes a scheme assisted by a reconfigurable intelligent surface (RIS) for efficient uplink traffic multiplexing between enhanced mobile broadband (eMBB) and ultra-reliable-low-latency communication (URLLC). The scheme determines two RIS configurations based only on the eMBB channel state information (CSI) available at the base station (BS). The first optimizes eMBB quality of service, while the second reduces eMBB interference in URLLC traffic by temporarily silencing the eMBB traffic. Numerical results demonstrate that this approach, relying solely on eMBB CSI and without BS coordination, can outperform the state-of-the-art preemptive puncturing by 4.9 times in terms of URLLC outage probability.

Index Terms

Reconfigurable intelligent surface (RIS), enhanced mobile broadband (eMBB), ultra-reliable low-latency communications (URLLC), and multiplexing.

I. INTRODUCTION

The fifth generation (5G) of mobile networks have been launched with features to support heterogeneous services with different quality of service (QoS) requirements and traffic char-

This work has been submitted to the IEEE for possible publication. Copyright may be transferred without notice, after which this version may no longer be accessible.

J. H. Inacio de Souza and T. Abrão are with the Department of Electrical Engineering, Universidade Estadual de Londrina, Brazil (e-mail: joahis@outlook.com, taufik@uel.br).

V. Croisfelt, R. Kotaba, and P. Popovski are with the Department of Electronic Systems, Aalborg University, Denmark (e-mail: {vcr,rak,petarp}@es.aau.dk).

acteristics [1]. In particular, enhanced mobile broadband (eMBB) services require extremely high spectral efficiency (SE), while ultra-reliable-low-latency communication (URLLC) services demand high reliability and low latency [2]. Due to these very different QoSs, there is a need for new multiplexing strategies that perform effectively in challenging channel conditions and better accommodate heterogeneous traffic demands from both eMBB and URLLC services.

An reconfigurable intelligent surface (RIS) is a thin sheet of composite material that can cover, *e.g.*, parts of walls and buildings. It can reflect incident signals to desired directions by dynamically configuring the phase shifts of the many elements that compose it [3]. In the literature, works like [4]–[6] study the fundamental limits and optimize the QoS in RIS-assisted URLLC applications. Our work is motivated by the fact that RIS can help to deliver the QoS for heterogeneous services, an aspect that has received less attention in the research literature.

Regarding heterogeneous traffic multiplexing, 5G new radio (5G NR) has introduced the *preemptive puncturing scheme*, that relies on base station (BS) coordination to interrupt the eMBB traffic and prioritizes the URLLC transmissions [7], [8]. Despite its fair downlink (DL) performance, in the uplink (UL), such a strategy increases the URLLC latency, mainly due to the waiting time for the BS to grant scheduling responses. Meanwhile, in the case of RIS-assisted systems, the multiplexing of eMBB/URLLC services gives rise to two additional challenges [8]. First, the BS is unaware of the time of arrival of a URLLC packet and cannot estimate its channel state information (CSI) to tailor the RIS configuration [2]. Second, controlling the RIS adds extra overhead that can violate the URLLC latency requirements.

For the DL, some of the deployment issues associated with RIS can be mitigated through the RIS configurations and resource allocation policies proposed in [9]–[11]. In contrast, for the UL, [12] suggests RIS configuration designs to aid both eMBB and URLLC user’s equipment (UE) even when URLLC CSI is unavailable, using non-orthogonal multiple access (NOMA) for service multiplexing. However, these studies still rely on heterogeneous multiplexing strategies that require BS coordination and may face challenges related to RIS control, without directly addressing the previously mentioned issues.

In this letter, we propose a new RIS-assisted multiplexing scheme to support heterogeneous eMBB and URLLC UL traffic. Rather than depending on BS coordination, our scheme is based on the assumption that the RIS is equipped with an antenna, and the RIS is then capable of minimally processing the signal received by this antenna to detect URLLC traffic. Then, inspired by the preemptive puncturing of 5G NR, the RIS multiplexes the services using two configurations,

which rely solely on eMBB CSI. The first assists the eMBB UE by optimizing the signal strength and thus its SE. The second, motivated by [13], is designed to assist the URLLC UE (if detected) by temporarily silencing the eMBB interference. The proposed scheme is compared to benchmarks in terms of outage probability for the URLLC service and SE for the eMBB. Numerical results show that the proposed scheme can outperform the outage probability of preemptive puncturing by 4.9 times.

II. SYSTEM MODEL

We consider a narrowband UL channel of a wireless system with one single-antenna BS, one hybrid RIS, and two single-antenna UEs, where the BS controls the RIS via an out-of-band control channel [14]. One of the UE uses the eMBB service, while the other uses the URLLC one.¹ Henceforth, we index the UEs by $\iota \in \{e, u\}$, where e and u refer to eMBB and URLLC, respectively. We assume an industrial scenario where the line-of-sight (LoS) between the BS and the UEs is blocked by obstacles. Thus, the RIS is deployed to simultaneously have LoS to the BS and the UEs. The RIS is a square uniform planar array (UPA) of $N \in \mathbb{Z}_+$ half-wavelength spaced passive reflecting elements and one active element, placed at the center of the RIS. The RIS can perform light computational tasks by processing the signal received by its active element. Each passive element can induce a phase shift $\theta_n \in [0, 2\pi)$ to an impinging signal with marginal impact on its amplitude. On this basis, we define an RIS configuration as $\boldsymbol{\psi} = [\psi_1 \cdots \psi_N]^T$, where $\psi_n = e^{-j\theta_n}$ is the reflection coefficient of the n -th RIS element.

A. Structure of a Uplink Frame

Fig. 1 depicts a UL frame, in which the time-frequency resources used by the UEs are organized into a grid. In the time domain, the length of the UL frame is $T > 0$, and it is divided into $M \in \mathbb{Z}_+$ identical mini-slots of duration $T_m > 0$, which are indexed by $\mathcal{M} = \{1, \dots, M\}$. In the frequency domain, the spectrum reserved for UL has the bandwidth $B > 0$. Due to different requirements, the UEs have different transmission time intervals (TTIs). To achieve high SE, the eMBB TTI spans over the entire frame. Conversely, the URLLC TTI spans over a limited number of $M_u \in \mathbb{Z}_+$, $1 \leq M_u \leq M$ contiguous mini-slots to guarantee the low-latency requirement. We

¹To attain efficient multi-user communication, it is common to multiplex several UEs of each traffic type in a wideband channel. However, to simplify the analysis, we consider a single UE of each traffic type in a narrowband channel, leaving the general case for a future extension of this work.

denote as $\mathcal{M}_u \subseteq \mathcal{M}$ with $|\mathcal{M}_u| = M_u$ the set of mini-slots of the URLLC TTI. Moreover, we consider that the eMBB UE is admitted and scheduled by the BS at the frame start, while the URLLC UE can start transmitting at any mini-slot.

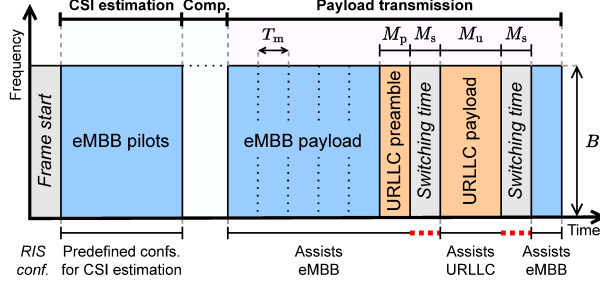


Fig. 1. UL frame divided into CSI estimation, computing, and payload transmission.

B. Signal Model

Let the vector $\mathbf{h}_b \in \mathbb{C}^N$ denotes the BS-RIS channels and the vectors $\mathbf{h}_l \in \mathbb{C}^N$ denote the RIS-UEs channels. We further assume the block-fading model, *i.e.*, the channels remain constant for the entire frame duration. Therefore, the BS-UEs cascaded channels are represented by the vector [13]

$$\mathbf{g}_l \triangleq \text{diag}(\mathbf{h}_b) \mathbf{h}_l. \quad (1)$$

Finally, we let the scalars $g_{l,n} = [\mathbf{g}_l]_n$ denote the BS-UEs cascaded channels that pass through the n -th RIS element. We denote as $\mathbf{x}_{l,m} \in \mathbb{C}^L$ the vectors with the $L \in \mathbb{Z}_+$ symbols transmitted by each UE such that $\mathbb{E}\{\|\mathbf{x}_{l,m}\|_2^2\} = 1$ in the m -th mini-slot. Thus, $\mathbf{x}_{u,m} = \mathbf{0}$ in the mini-slots with absence of URLLC traffic, that is, when $m \notin \mathcal{M}_u$. Let $p_l > 0$ denote the UEs' transmit power for one mini-slot. Considering the RIS configuration $\boldsymbol{\psi}$, the received signal $\mathbf{y}_m(\boldsymbol{\psi}) \in \mathbb{C}^L$ at the BS can be written as:

$$\mathbf{y}_m(\boldsymbol{\psi}) \triangleq \sqrt{p_u}(\mathbf{g}_u^H \boldsymbol{\psi}) \mathbf{x}_{u,m} + \sqrt{p_e}(\mathbf{g}_e^H \boldsymbol{\psi}) \mathbf{x}_{e,m} + \mathbf{w}_m, \quad (2)$$

where $\mathbf{w}_m \sim \mathcal{CN}(\mathbf{0}, \sigma^2 \mathbf{I})$ is the additive white Gaussian noise (AWGN). Using (2), the signal-to-noise ratio (SNR) for the eMBB UE in the mini-slots without URLLC traffic is:

$$\Gamma_{e,m}(\boldsymbol{\psi}) \triangleq p_e |\mathbf{g}_e^H \boldsymbol{\psi}|^2 / \sigma^2, \quad \forall m \in \mathcal{M} \setminus \mathcal{M}_u. \quad (3)$$

Also, during the URLLC TTI, the signal-to-interference-plus-noise ratio (SINR) for the URLLC UE is given by

$$\Gamma_{u,m}(\boldsymbol{\psi}) \triangleq p_u |\mathbf{g}_u^H \boldsymbol{\psi}|^2 / (p_e |\mathbf{g}_e^H \boldsymbol{\psi}|^2 + \sigma^2), \quad \forall m \in \mathcal{M}_u. \quad (4)$$

With (3) and (4), one can measure the quality of the radio links established for the UEs by the RIS.

III. RIS-ASSISTED MULTIPLEXING SCHEME

Here, we introduce our proposed multiplexing scheme. First, we explain the three phases comprising a UL frame and give an overview of how our scheme works. Then, we discuss how the RIS could detect the URLLC traffic, and we parameterize the performance of an arbitrary detector by its miss detection rate, ϵ_m . Finally, to multiplex the eMBB and URLLC services, we design two RIS configurations that rely only on eMBB CSI.

A. Phases of the Multiplexing Scheme

From Fig. 1, a UL frame is divided into three phases. **1. CSI Estimation:** The BS estimates the eMBB CSI by using pilot symbols sent by the eMBB UE, while the RIS switches among predefined configurations (for more details, see [3]). **2. Computing:** The BS computes two RIS configurations based on the eMBB CSI, the *eMBB-oriented configuration* and the *URLLC-oriented configuration* to potentially multiplex the eMBB and URLLC services within the given frame. Finally, these two configurations are sent to the RIS to be stored there for potential use in the next phase. **3. Payload Transmission:** In this phase, the scheduled eMBB UE transmits its payload whereas the RIS starts by being configured with the eMBB-oriented configuration. At any time in this phase, if the URLLC UE has a packet to send, it will start its TTI by sending a preamble over $M_p \in \mathbb{Z}_+$ mini-slots to announce its intention to transmit payload data. By exploiting its active element² and the URLLC preamble, the RIS can *detect* the start of the URLLC traffic. If URLLC traffic is detected, the RIS switches to the URLLC-oriented configuration to multiplex the URLLC TTI; otherwise, it keeps the eMBB-oriented configuration. In the former case, when the URLLC TTI is over, the RIS switches back to the eMBB-oriented configuration. Note that while all this occurs, the eMBB TTI is not interrupted, so part of the eMBB mini-slots will be erased by the URLLC traffic, and by the changes in the environment caused by the RIS.³

²In practice, this active element could also be the antenna of the communication interface used to control the RIS [3], making it a viable solution.

³To decode the eMBB payload data at the BS with a limited number of erased mini-slots, erasure coding can be applied by the eMBB UE [2].

In practice, the RIS can impose a physical latency due to switching configurations. By assuming that the time the RIS takes to change its phase shifts is around some microseconds [3], we consider the RIS takes $M_s \in \mathbb{Z}_+$ mini-slots to switch between configurations. We also assume that the URLLC UE is aware of this *switching time* and waits for it before transmitting the payload. Hence, in case the URLLC traffic is detected, the RIS adds an overhead of M_s mini-slots for the URLLC UE and $2M_s$ mini-slots for the eMBB one.

B. Detecting the URLLC Traffic

The URLLC traffic can be identified at the RIS using the preamble signaling spanning over M_p mini-slots. To do so, one effective approach would involve the joint design of the preamble and detection algorithm to meet URLLC QoSs. For instance, in the context of URLLC service, a robust scheme presented in [15] introduces a brief preamble consisting of a single orthogonal frequency-division multiplexing (OFDM) symbol, detected at the receiver using differential detection. This algorithm can be seamlessly implemented in a hybrid RIS with limited signal processing capacity. However, we investigate the performance of an arbitrary detection scheme, assessing its general impact on multiplexing efficiency without relying on a specific scheme. We parameterize the performance of this detector by its *miss detection rate*, defined as $0 \leq \epsilon_m \leq 1$, whose impact is evaluated in Section V.

C. Computing the eMBB-Oriented RIS Configuration

The eMBB-oriented RIS configuration $\boldsymbol{\psi}^e \in \mathbb{C}^N$ is set to maximize the eMBB SNR, which can be posed as the following optimization problem

$$\max_{\boldsymbol{\psi} \in \mathbb{C}^N} |\mathbf{g}_e^H \boldsymbol{\psi}|^2 / \sigma^2, \text{ s.t. } \mathbf{C}_1 : |\psi_n| = 1, \forall n \in \{1, \dots, N\}. \quad (5)$$

Fortunately, this problem assumes a family of closed-form solutions known as coherent passive beamformers [14]. Based on this and with eMBB CSI,⁴ $\boldsymbol{\psi}^e$ can be computed as:

$$\boldsymbol{\psi}^e = [e^{-j\theta_1^e} \ \dots \ e^{-j\theta_N^e}]^T, \text{ where} \quad (6)$$

$$\theta_n^e = -\arg(g_{e,n}) + \bar{\theta}, \ n \in \{1, \dots, N\},$$

⁴We assume perfect CSI knowledge at the BS to show the upper bound performance of the proposed scheme, leaving the study of the impact of imperfect CSI for future work.

and $\bar{\theta} \in [0, 2\pi)$ due to the phase periodicity. For the sake of simplicity but without compromising generality, we take $\bar{\theta} = 0$. In such a case, from (1), the effective channel of the eMBB UE can be simplified to $\mathbf{g}_e^H \boldsymbol{\psi}^e = \sum_{n=1}^N |g_{e,n}|$. Hence, the RIS yields the maximum array gain of N^2 , providing high SE.

D. Computing the URLLC-Oriented RIS Configurations

At the BS, the computation of an RIS configuration to multiplex the URLLC TTI is challenging since only eMBB CSI is available at the BS. Our idea is to find a configuration that mitigates the interference caused by the eMBB traffic to the URLLC one, that is, that temporarily silences the eMBB UE. We present two methods for computing the URLLC-oriented configuration. The first one is a heuristic based on *phasors rotation* that tries to cancel out the channel gain of the eMBB UE by compensating the phase shifts of the RIS elements via subtraction. The second one is an *alternating projection* algorithm to approximate a configuration that nulls the eMBB interference.

Method 1: Phasors rotation (PR). Given the eMBB CSI, let us define the problem of finding an RIS configuration that minimizes the channel gain of the eMBB UE as

$$\min_{\boldsymbol{\psi} \in \mathbb{C}^N} |\mathbf{g}_e^H \boldsymbol{\psi}|, \text{ s.t. } C_1, \quad (7)$$

with C_1 as in (5), which makes the problem to be not convex. However, notice that the channel gain is lower-bounded such that $|\mathbf{g}_e^H \boldsymbol{\psi}| \geq 0$. Therefore, our goal is to find a configuration that make this gain as close as possible to zero.

We start by presenting a heuristic algorithm with low computational complexity, which yields a sub-optimal solution to problem (7). The heuristic is based on the representation of the eMBB cascaded channels as phasors, and the idea that we can individually rotate them so that they cancel each other out, nulling the eMBB channel. This is made by dividing the RIS elements into two sets, where the goal of one of the sets is to eliminate the contribution of the other. From (1), let the n -th eMBB cascaded channel reflected by the RIS be represented by the phasor such that

$$A_n e^{j\omega_n} \triangleq g_{e,n}^* \boldsymbol{\psi}_n, \quad (8)$$

where $A_n = |g_{e,n}|$ is the phasor's amplitude, and $\omega_n = -\arg(g_{e,n}) - \theta_n$ is the phasor's angle. Let the nonempty sets \mathcal{N}_0 and \mathcal{N}_π denote a partition of the RIS elements, *i.e.* $\mathcal{N}_0 \cup \mathcal{N}_\pi = \{1, \dots, N\}$

and $\mathcal{N}_0 \cap \mathcal{N}_\pi = \emptyset$. The RIS elements are configured with the following phase shift according to the set they belong

$$\theta_n^u = \begin{cases} -\arg(g_{e,n}), & n \in \mathcal{N}_0 \\ \pi - \arg(g_{e,n}), & n \in \mathcal{N}_\pi \end{cases}. \quad (9)$$

Using the configuration $\boldsymbol{\psi}^u = [e^{-j\theta_1^u} \dots e^{-j\theta_N^u}]^\top$, the cascaded channels belonging to sets \mathcal{N}_0 and \mathcal{N}_π are out of phase, since $\omega_n = 0$ if $n \in \mathcal{N}_0$ and $\omega_n = -\pi$ if $n \in \mathcal{N}_\pi$. Therefore, from (8) and (9), the eMBB channel gain with $\boldsymbol{\psi}^u$ is equal to

$$|\mathbf{g}_e^H \boldsymbol{\psi}^u| = \left| \sum_{n=1}^N A_n e^{j\omega_n} \right| = \left| \sum_{n \in \mathcal{N}_0} A_n - \sum_{n' \in \mathcal{N}_\pi} A_{n'} \right|. \quad (10)$$

Thus, to mitigate the interference caused by the eMBB traffic, we need to determine the sets \mathcal{N}_0 and \mathcal{N}_π that approximately null (10). Since each cascaded channel can belong to either \mathcal{N}_0 or \mathcal{N}_π , minimizing (10) is a combinatorial optimization problem with 2^N candidate solutions. As this is not tractable even for moderate size RISs, in Algorithm 1 we present an intuitive method for determining \mathcal{N}_0 and \mathcal{N}_π , approximating a solution that minimizes (10) in feasible computation time.

Algorithm 1 Phasors rotation algorithm.

input: The channel vector \mathbf{g}_e

output: The RIS configuration $\boldsymbol{\psi}^u$

- 1: $A_n \leftarrow |g_{e,n}|$
 - 2: $(\alpha_i)_{i=1}^N \leftarrow \text{sort}(A_1, \dots, A_N)$
 - 3: $N^* \leftarrow \arg \min \{ |\sum_{i=1}^{N'} \alpha_i - \sum_{i'=N'+1}^N \alpha_{i'}| \mid 1 \leq N' \leq N \}$
 - 4: $\mathcal{N}_0 \leftarrow \{\mu(1), \dots, \mu(N^*)\}$, $\mathcal{N}_\pi \leftarrow \{\mu(N^* + 1), \dots, \mu(N)\}$
 - 5: Set θ_n^u , $\forall n \in \{1, \dots, N\}$ according to eq. (9)
 - 6: **return** $\boldsymbol{\psi}^u \leftarrow [e^{-\theta_1^u} \dots e^{-\theta_N^u}]^\top$
-

The algorithm works as follows. Initially, the amplitudes of the phasors representing the cascaded channels are computed. Then, the algorithm finds an integer number $1 \leq N^* \leq N$ such that the sum of the amplitudes of the N^* shortest phasors is as close as possible to the sum of the amplitudes of the $N - N^*$ remaining ones. Finally, the set \mathcal{N}_0 is created with the indices of the elements associated with the N^* shortest phasors, while \mathcal{N}_π is created with the indices of the remaining ones. In the algorithm, $\mu(\cdot)$ maps the indices of $(\alpha_i)_{i=1}^N$ to $\{A_n\}_{n=1}^N$.

Method 2: Interference Nulling (IN). The second method of finding an RIS configuration that nulls the eMBB interference at the BS can be cast as the following feasibility problem

$$\text{find } \boldsymbol{\psi} \in \mathbb{C}^N, \text{ s.t. } C_1 \text{ and } C_2 : \mathbf{g}_e^H \boldsymbol{\psi} = 0, \quad (11)$$

where C_1 is defined as in (5), while C_2 ensures that the eMBB traffic does not interfere at the BS. Similarly to (7), this problem is not convex due to the unit modulus constraints C_1 . However, notice that, if any, a solution to the problem is any vector that belongs to the intersection between the sets defined by constraints C_1 and C_2 . In this case, the alternating projection algorithm can approximate a solution with a high probability of convergence. In this sense, Algorithm 2 presents an adaption of the alternating projection algorithm in [13] that iteratively approximates a solution to problem (11). During each iteration $t \in \mathbb{Z}_+$, the vector of reflection coefficients $\boldsymbol{\psi}_{t-1}$ is projected sequentially onto the set $\{\boldsymbol{\psi} \in \mathbb{C}^N \mid \mathbf{g}_e^H \boldsymbol{\psi} = 0\}$, then onto the set $\{\boldsymbol{\psi} \in \mathbb{C}^N \mid |\psi_n| = 1, \forall n \in \{1, \dots, N\}\}$. The projection operators consider the smallest Euclidean distance from $\boldsymbol{\psi}_{t-1}$ to a point in the projected set, derived according to [13, eq. (20)]. We use early stopping and maximum iterations as stopping criteria.

Algorithm 2 Alternating projection algorithm for IN.

input: The channel vector \mathbf{g}_e and the initial configuration $\boldsymbol{\psi}_0$

output: The RIS configuration $\boldsymbol{\psi}^u$

- 1: $\mathbf{v} \leftarrow \mathbf{g}_e / \|\mathbf{g}_e\|_2, t \leftarrow 1$
 - 2: **repeat**
 - 3: $\tilde{\boldsymbol{\psi}} \leftarrow \boldsymbol{\psi}_{t-1} - (\mathbf{v}^H \boldsymbol{\psi}_{t-1}) \mathbf{v}$
 - 4: $\boldsymbol{\psi}_t \leftarrow [\tilde{\psi}_1 / |\tilde{\psi}_1| \cdots \tilde{\psi}_N / |\tilde{\psi}_N|]^T$
 - 5: $t \leftarrow t + 1$
 - 6: **until** stopping criterion is satisfied
 - 7: **return** $\boldsymbol{\psi}^u \leftarrow \boldsymbol{\psi}_{t-1}$
-

IV. ANALYSIS

This section introduces the metrics used to analyze the proposed multiplexing scheme.

Performance Analysis: By using the RIS configurations of Section III, we present expressions for the outage probabilities achieved by the eMBB and URLLC UEs. Initially, considering the

configuration $\boldsymbol{\psi}^e$ in (6), the instantaneous mutual information per mini-slot of the eMBB data stream at the BS is:

$$\begin{aligned} I_e(p_e) &\triangleq M^{-1} \sum_{m=1}^M (1 - \xi) \log_2(1 + \Gamma_{e,m}(\boldsymbol{\psi}^e)), \\ &= (1 - \xi) \log_2(1 + p_e(\sum_{n=1}^N |g_{e,n}|)^2/\sigma^2), \end{aligned} \quad (12)$$

where the pre-log term $\xi = (M_p + 2M_s + M_u)/M$ accounts for the mini-slots of the URLLC TTI and RIS configuration switching. Similarly, the instantaneous mutual information per mini-slot of the URLLC data stream considering the RIS configuration $\boldsymbol{\psi}^u$ computed by Algorithms 1 or 2 is derived as

$$\begin{aligned} I_u(p_u, p_e) &\triangleq M_u^{-1} \sum_{m \in \mathcal{M}_u} \log_2(1 + \Gamma_{u,m}(\boldsymbol{\psi}^u)), \\ &= \log_2(1 + p_u |\mathbf{g}_u^H \boldsymbol{\psi}^u|^2 / (p_e |\mathbf{g}_e^H \boldsymbol{\psi}^u|^2 + \sigma^2)). \end{aligned} \quad (13)$$

Therefore, given constant transmit power, the outage probabilities of the eMBB and URLLC UEs as functions of the SEs per mini-slot, $r_l > 0$, are respectively equal to

$$P_e(r_e) \triangleq \Pr(I_e(p_e) < r_e) \text{ and } P_u(r_u) \triangleq \Pr(I_u(p_u, p_e) < r_u).$$

Latency Analysis: From Fig. 1, the latency introduced by the proposed scheme to the URLLC traffic is governed by: **a)** the transmission of the URLLC preamble, **b)** the delay due to processing of the preamble and switching between configurations at the RIS, and **c)** the transmission of the URLLC payload symbols. Neglecting the propagation delay, the latency introduced by the transmission of the URLLC preamble and payload are respectively $M_p T_m$ and $M_u T_m$. Moreover, we let $D_{\text{proc}} > 0$ be a constant that accounts for the time needed to process the preamble at the RIS and detect the URLLC traffic. Also, recall that the delay for the RIS to switch to the URLLC-oriented configuration is $M_s T_m$. Then, the URLLC latency is:

$$D = M_p T_m + M_u T_m + D_{\text{proc}} + M_s T_m. \quad (14)$$

If the processing delay is negligible compared to the mini-slot duration, a reasonable approximation for the URLLC latency is $D \approx (M_p + M_s + M_u) T_m$. As a comparison, in the 5G NR preemptive puncturing, the latency increases in the order of the slot duration due to the BS coordination [7]. Due to space limitations, we leave a detailed comparison for future work.

V. NUMERICAL RESULTS

Now, we present numerical simulations to discuss the performance of the proposed scheme for multiplexing eMBB and URLLC services. In the simulations, \mathbf{h}_b and \mathbf{h}_t follow the line-of-sight channel model in [16, eqs. (6) and (7)], with $\lambda = 0.1$ m, $\beta = 3.67$, $\gamma_0 = 1$, $d_0 = 1$ m, and $\sigma^2 = -90$ dBm.⁵ Moreover, we consider $M_p = M_s = 1$ mini-slot and $M_u = 2$ mini-slots. The RIS is a square surface placed at the origin of the coordinate system in the yz -plane, pointing towards the direction of the x -axis. The BS is at $\mathbf{q}_{\text{BS}} = [\varrho_f/\sqrt{2} \ \varrho_f/\sqrt{2} \ 0]^T$, where $\varrho_f = \lambda(\sqrt{N} - 1)^2/2$ is the far-field distance of the RIS. The region occupied by the UEs is a volume defined in spherical coordinates by the set $\{(\varrho, \vartheta, \varphi) \mid \varrho_f \leq \varrho \leq 100 \text{ m}, \vartheta_{\min} \leq \vartheta \leq \vartheta_{\max}, \frac{3\pi}{2} \leq \varphi \leq 2\pi\}$, where the tuple $(\varrho, \vartheta, \varphi)$ denotes, respectively, the radial distance, the polar, and azimuthal angles. Specifically, the angles $\vartheta_{\min}, \vartheta_{\max}$ are such that the z -coordinates of the UEs lie within $[-3, 3]$ m. The UEs' positions, drawn for each 10^7 realization, are uniformly distributed over this region.

Benchmarks: To compare the proposed algorithms for computing the URLLC-oriented configuration, we define the following benchmarks: **a) Random:** The phase shifts $\{\theta_n^u\}_{n=1}^N$ are drawn from a uniform distribution over the interval $[0, 2\pi)$. **b) Missed URLLC preamble:** eMBB-oriented configuration, representing the case where the RIS always fails to detect the start of the URLLC traffic ($\epsilon_m = 1$).⁶ **c) Preemptive puncturing:** Following the procedure described in [7], the eMBB TTI is interrupted so as the URLLC UE has an interference-free TTI. Still, since there is no URLLC CSI knowledge at the BS, the RIS keeps the eMBB-oriented configuration. **d) Maximize URLLC SNR:** Ideally, assuming that URLLC CSI is available at the BS prior to its TTI, ψ^u is set to perform coherent passive beamforming like in (6), but for the URLLC UE.

Figs. 2a and 2b present the URLLC outage probability as a function of the SE and the transmit power ratio, respectively. These results reveal the gains of the proposed PR and IN algorithms over the benchmarks, even relying only on eMBB CSI. Notice that the PR and IN performance is comparable to the preemptive puncturing, where there is no eMBB interference due to the BS scheduling. Remarkably, the IN algorithm outperforms the preemptive puncturing performance by 4.9 times in Fig. 2b. Compared to the random and the PR configurations, interference nulling

⁵The operations of the proposed algorithms and benchmarks are independent of the channel model, applying to other, more general, models.

⁶The benchmarks **a)** and **b)** are respectively equivalent to the configurations to assist the URLLC and eMBB UEs in [12].

(IN) reduces the outage probability by up to 3 orders of magnitude and 3.5 times, respectively. However, the PR algorithm yields a better trade-off due to its simpler implementation.

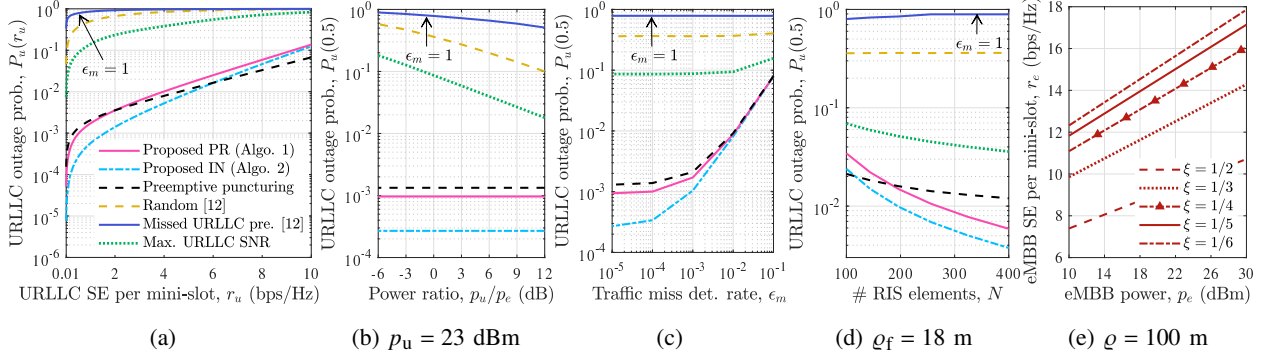


Fig. 2. URLLC outage probability and eMBB SE at the cell edge. When not otherwise specified, the transmit powers are $p_e = p_u = 23$ dBm, the RIS has $N = 100$ elements, the URLLC traffic miss detection rate is $\epsilon_m = 0$, and the RIS far-field distance is $\varrho_f = 4$ m. Also, in (e), ξ is the fraction of eMBB mini-slots unaffected by the URLLC TTI and the RIS switching, as defined in (12).

Fig. 2c depicts the URLLC outage probability as a function of the URLLC traffic miss detection rate. Only for preemptive puncturing, ϵ_m is considered to be the failure rate for the URLLC scheduling request procedure. Notice that, for the proposed scheme, the traffic detection scheme is not considered a major limiting factor for the performance, mainly because there are simple architectures for it that yield extremely low detection error rates. For example, a scheme in [13] achieves a detection error rate of up to 10^{-7} at an SNR of 4 dB with a preamble comprised by a single OFDM symbol.

Fig. 2d depicts the URLLC outage probability as a function of the number of RIS elements. It is worth mentioning that, as the outage probability improves with a bigger surface, the overhead for estimating the eMBB CSI increases proportionally to N . Hence, when selecting the number of RIS elements, a trade-off exists between the URLLC outage probability and the overhead in the CSI estimation phase.

Fig. 2e depicts the SE of the eMBB UE when placed at the cell edge ($\varrho = 100$ m) as a function of the transmit power. Notice that, as the URLLC packet size is relatively small compared to the eMBB, the mini-slots erased by the URLLC traffic have minimal impact on the eMBB TTI, resulting in high eMBB SE.

VI. CONCLUSIONS

In this letter, we have proposed an RIS-assisted UL multiplexing scheme to support the eMBB/URLLC coexistence. The scheme relies on two RIS configurations computed from eMBB CSI. The first configuration is a coherent passive beamformer to maximize the eMBB SNR. The second is computed by the proposed PR and IN algorithms and mitigates the eMBB interference in the URLLC traffic, temporarily silencing the eMBB traffic. Numerical results have demonstrated that the proposed scheme enables a balanced coexistence of the services in the absence of URLLC CSI.

REFERENCES

- [1] M. Z. Chowdhury *et al.*, “6G wireless communication systems: Applications, requirements, technologies, challenges, and research directions,” *IEEE Open J. of the Commun. Society*, vol. 1, pp. 957–975, July 2020.
- [2] P. Popovski *et al.*, “5G wireless network slicing for eMBB, URLLC, and mMTC: A communication-theoretic view,” *IEEE Access*, vol. 6, pp. 55 765–55 779, Sept. 2018.
- [3] M. Di Renzo *et al.*, “Smart radio environments empowered by reconfigurable intelligent surfaces: How it works, state of research, and the road ahead,” *IEEE J. on Sel. Areas in Commun.*, vol. 38, no. 11, pp. 2450–2525, July 2020.
- [4] H. Xie *et al.*, “User grouping and reflective beamforming for IRS-aided URLLC,” *IEEE Wireless Commun. Lett.*, vol. 10, no. 11, pp. 2533–2537, Nov. 2021.
- [5] Z. Li *et al.*, “Resource allocation for IRS-assisted uplink URLLC systems,” *IEEE Commun. Lett.*, Apr. 2023, early access.
- [6] H. Ren *et al.*, “Intelligent reflecting surface-aided URLLC in a factory automation scenario,” *IEEE Trans. on Commun.*, vol. 70, no. 1, pp. 707–723, Jan. 2022.
- [7] “NR and NG-RAN overall description,” *document 3GPP TS 38.300 V17.5.0*, June 2023.
- [8] M. Almekhlafi *et al.*, “Enabling URLLC applications through reconfigurable intelligent surfaces: Challenges and potential,” *IEEE Internet of Things Mag.*, vol. 5, no. 1, pp. 130–135, Mar. 2022.
- [9] H. Zarini *et al.*, “Resource management for multiplexing eMBB and URLLC services over RIS-aided THz communication,” *IEEE Trans. on Commun.*, pp. 1–15, Jan. 2023, early access.
- [10] M. Almekhlafi *et al.*, “Joint resource allocation and phase shift optimization for RIS-aided eMBB/URLLC traffic multiplexing,” *IEEE Trans. on Commun.*, vol. 70, no. 2, pp. 1304–1319, Feb. 2022.
- [11] W. R. Ghanem *et al.*, “Codebook based two-time scale resource allocation design for IRS-assisted eMBB-URLLC systems,” in *2022 IEEE Globecom Workshops (GC Wkshps)*, 4–8 Dec. 2022, pp. 419–425.
- [12] V. D. P. Souto *et al.*, “IRS-aided physical layer network slicing for URLLC and eMBB,” *IEEE Access*, vol. 9, pp. 163 086–163 098, Dec. 2021.
- [13] T. Jiang and W. Yu, “Interference nulling using reconfigurable intelligent surface,” *IEEE J. on Sel. Areas in Commun.*, vol. 40, no. 5, pp. 1392–1406, May 2022.
- [14] E. Björnson *et al.*, “Reconfigurable intelligent surfaces: A signal processing perspective with wireless applications,” *IEEE Signal Process. Mag.*, vol. 39, no. 2, pp. 135–158, Mar. 2022.
- [15] X. Jiang *et al.*, “Packet detection by a single OFDM symbol in URLLC for critical industrial control: A realistic study,” *IEEE J. on Sel. Areas in Commun.*, vol. 37, no. 4, pp. 933–946, Apr. 2019.

- [16] A. Albanese *et al.*, “MARISA: A self-configuring metasurfaces absorption and reflection solution towards 6G,” in *IEEE INFOCOM 2022 - IEEE Conf. on Comput. Commun.*, 2-5 May 2022, pp. 250–259.